Syneresis of self-crowded calcium-alginate hydrogels as a self-driven athermal aging process. — Supplementary Information—

Bruno Da Silva Pinto, Tristan Baumberger & Olivier Ronsin

1 The optical front is actually a gelation front — video

Video movie CORESHELL.mp4 (10× speed) — 10 wt.% sodium alginate extruded in a 100 mM calcium chloride bath. The steel needle has a inner diameter 840 μm. In response to a non-steady extrusion velocity history the diameter of the fibre is not uniform (rate-controlled viscoelastic "dye-swelling"). The white curves travelling from the fibre boundary towards the axis, made brighter by slightly defocussing the objective, define an optical front the diameter of which is not uniform either. A large air bubble, initially trapped into the syringe, was co-extruded with the fibre. Due to buoyancy and fibre-asymmetry it moves upward. No relative flow is observed in the outside shell. This clearly identifies the optical surface as a gelation front separating a solid gel shell from a liquid pregel core.

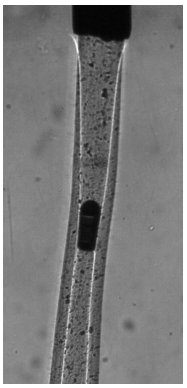

Figure 1 Snapshot of CORESHELL.mp4 movie. See description in the text.

2 A minimal model for the gelation of an alginate fiber

In this section, we describe the minimal model used to analyse the kinetics of calcium induced gelation of an alginate cylinder (section 3.1.1 of the manuscript). For simplicity, we denote here the time t rather than t_1. Following Chavez et al.[1], we assume that (i) only Ca^{2+} ions diffuse from the $CaCl_2$ bath through the gelled alginate, to the gelation front of radius $r_f(t)$, and (ii) gelation there is assumed instantaneous.

In cylindrical coordinates, noting $c(r,t)$ the Ca^{2+} concentration inside the alginate gel shell and $\mathscr{D}_{\rm ion}$ the diffusion coefficient, the diffusion equation reads:

$$\frac{\partial c}{\partial t} = \frac{\mathscr{D}_{\rm ion}}{r}\frac{\partial}{\partial r}\left(r\frac{\partial c}{\partial r}\right) \tag{1}$$

with the boundary conditions (see Figure 2):

$$c(R_0,t) = c_0 \tag{2}$$

at the interface with the $CaCl_2$ bath,

$$c(r_f(t),t) = 0 \tag{3}$$

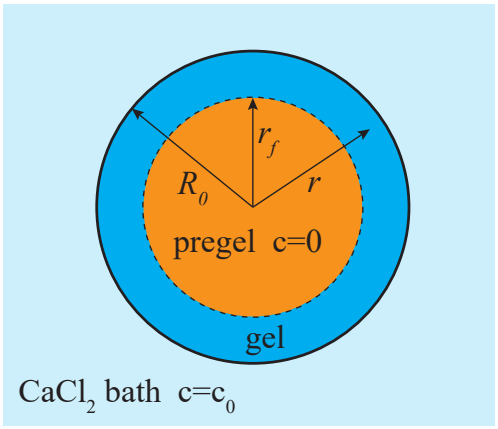

Figure 2 Cylindrical geometry of the alginate thread immersed in a $CaCl_2$ bath. Calcium ions diffuse through the shell of gelled alginate to the pregel interface where the can react to make the front advance.

at the interface with the alginate solution, and with an initial value

$$r_f^0 = r_f(t=0) = R_0. \tag{4}$$

At the gelation front $r = r_f(t)$, per unit length of cylindrical fiber, the flux of Ca^{2+} ions $-2\pi r_f \mathscr{D}_{\rm ion}\nabla c|_{\rm r=r_f}$ provokes the gelation of a volume $-n\frac{d}{dt}(\pi r_f^2)$ of pregel, where n is the amount of ions per unit volume required to complete cross-linking. The front velocity is therefore

$$v_f = \frac{dr_f}{dt} = -\frac{\mathscr{D}_{\rm ion}}{n}\left.\frac{\partial c}{\partial r}\right|_{\rm r=r_f} \tag{5}$$

2.1 Quasi-stationary solution

When $n \ll c_0$, the front velocity is small and the concentration profile is quasi-stationary, from (1), (2) and (3):

$$c_{\rm qs}(r,t) = c_0\frac{\ln(r/r_f(t))}{\ln(R_0/r_f(t))}$$

The velocity of the gelation front is then, with (5)

$$\frac{dr_f}{dt} = -\frac{c_0\mathscr{D}_{\rm ion}}{n\ln(R_0/r_f)}\frac{1}{r_f}$$

With the initial condition $r_f(t=0) = R_0$, this integrates to

$$1 + \frac{r_f^2}{R_0^2}\left[2\ln\left(\frac{r_f}{R_0}\right) - 1\right] = \frac{4c_0\mathscr{D}_{\rm ion}t}{nR_0^2}$$

which can be rewritten in terms of the reduced front advance $\tilde{\rho}_f = 1 - r_f/R_0$:

$$\frac{1}{4} + \frac{(1-\tilde{\rho}_f)^2}{2}\left[\ln\left(1-\tilde{\rho}_f\right) - \frac{1}{2}\right] = \frac{c_0}{n}\frac{t}{\tau_{\rm ion}} \tag{6}$$

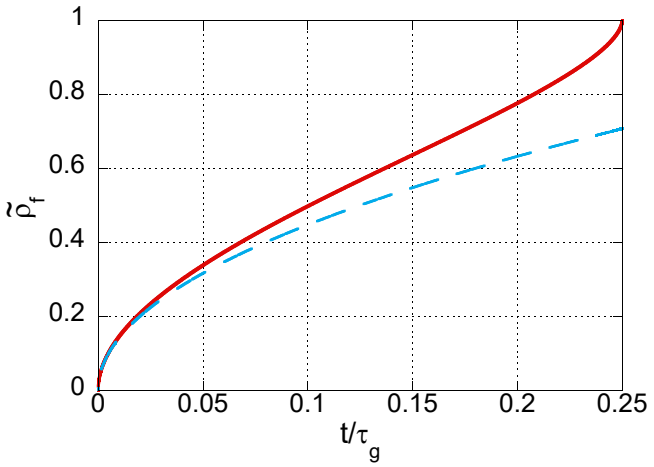

Figure 3 Full red curve : quasi-stationary evolution of the gelation front reduced position $\tilde{\rho}_f$ as a function of t/τ_g. Dotted blue curve : initial square root evolution.

with $\tau_{\text{ion}} = \dfrac{R_0^2}{\mathscr{D}_{\text{ion}}}$

At short times $t \ll n\tau_{\text{ion}}/c_0$, the front advance behaves as $\tilde{\rho}_f \simeq \sqrt{2t/\tau_g}$, with $\tau_{\text{ion}}/\tau_g = c_0/n$ whereas complete gelation of the fiber ($\tilde{\rho}_f = 1$) occurs at time $t_g = \tau_g/4$

2.2 Numerical solution

At larger bath concentrations, the gelation front velocity is too large for the quasi-stationary solution to remain valid. The diffusion equation must be solved numerically. We used a Cranck-Nicholson scheme[2] over a regular grid of size N (chosen between 10^3 and 10^6 without significant effect on the results), spanning the gelled shell. At each time step, $dt = 2\alpha dr^2/\mathscr{D}_{\text{ion}}$ with α a parameter chosen between 0.01 and 0.25 without significant effect on the results, we compute the instantaneous concentration profile. From this we extract the front velocity v_f using (5). The shell is increased accordingly. We then adapt the spatial grid step dr (keeping N constant) as well as the time step (keeping α constant). The concentration at new grid point is evaluated using second order polynomial interpolation.

This procedure requires a initial finite shell size d_0, with an initial concentration profile, and thus an initial value of the pregel region radius $r_f^0 = R_0 - d_0$, different from (4). However, with values of $d_0 \ll R_0$ (d_0/R_0 in the range 10^{-5}—10^{-3}), the precise concentration profile ($c(t=0,r) = 0$ or $c(t=0,r) = c_{\text{qs}}(r,t_0)$ with $r_f(t_0) = r_f^0$) only affects the front evolution on a time scale that remains negligible compared to τ_{ion}.

2.3 Results

The results presented in the following and in the manuscript where computed with $N = 1000$, $\alpha = 0.25$, and an initial shell thickness $d_0 = 10^{-3}R_0$ with an initial concentration profile corresponding to the quasi-stationary solution.

Figure 4 shows the evolution of the concentration profile with time for 4 different values of c_0/n, together (Fig.4.e) with the corresponding gelation front advance $\tilde{\rho}_f(t/\tau_{\text{ion}})$.

We find (Figure 4.e) that the initial front advance scales as $\tilde{\rho}_f \simeq \sqrt{2t/\tau_g}$. Figure 5.a shows that $\tau_{\text{ion}}/\tau_g = f(c_0/n)$ with $f(x) \simeq x$ when $x \ll 1$, recovering the quasi-stationary regime.

We can also extract the time t_g at which gelation is complete ($\tilde{\rho}_f(t_g) = 1$), and the ratio t_g/τ_g is found to depend slowly with c_0/n :

$$\frac{t_g}{\tau_g} = \frac{1}{4} g\left(\frac{c_0}{n}\right)$$

with $g(x) \simeq 1$ when $x \ll 1$ as shown on Figure 5.b, recovering the quasi-stationary regime.

3 Free counterion concentration in (pre)gels

Alginate is a negatively charged polyion bearing one charge per uronate residue of average length $b = 4.8$ Å. The charge density is conveniently assessed by the parameter ξ:

$$\xi = \frac{\ell_B}{b}$$

with ℓ_B the Bjerrum length ($\ell_B = 7.1$ Å in water at 293K):

$$\ell_B = \frac{e^2}{\varepsilon k_B T}$$

with e the elementary charge, ε the bulk dielectric constant of the solvant, k_B the Boltzmann constant and T the absolute temperature.

For alginate chains at room temperature $\xi \simeq 1.5$.

A wide corpus of experimental and theoretical studies[3] indicates that, due to long ranged Coulombic interactions, as ξ exceeds a critical value ξ_c, a fraction of the counterions are no longer free to diffuse into the solvent but perform restricted motion in the immediate vicinity of the polyion. They are said to be “condensed". The simplest theoretical model, i.e. an infinite line charge with point counterions of valence z, in the limit of vanishing concentrations, yield a critical density:

$$\xi_c = \frac{1}{z}$$

This value has been found compatible with numerous experimental properties of polyelectrolyte solutions exhibiting a threshold transition controlled by the charge density ξ.

The “limiting law" theory, usually referred to as Manning condensation theory[4] predicts that for $\xi > \xi_c$, counterions condense so as to neutralize polymer charges and reduce the charge density to its critical value. The concentration of condensed counterions of valence z is therefore $C_{\text{res}}\theta(z)$ with C_{res} the concentration of monovalent, polymer-bound charge sites and:

$$\theta(z) = \frac{1}{z}\left(1 - \frac{1}{z\xi}\right) \tag{7}$$

3.1 Sodium alginate pregels

In the sodium alginate pregel ($\xi = 1.5$, $z = 1$), condition (**??**) is fulfilled at room temperature irrespective of the polymer concentration. The molar mass of sodium uronates (M of G) being 256 Da,

$$C_{\text{res}} = C_A(wt.\%)\frac{10}{256}$$

This is also the total concentration of sodium ions in the solution, part of which are condensed, part of which are free to diffuse into the bulk of the pregel. In the following we will evaluate the concentrations of both counterion populations within the framework of Manning’s limiting law (7). These values must be taken with a pinch of salt due to the relatively large levels of ion concentrations (with respect to the validity of limiting laws in polyelectrolytes) used in the experimental study. We assume Manning’s theory to

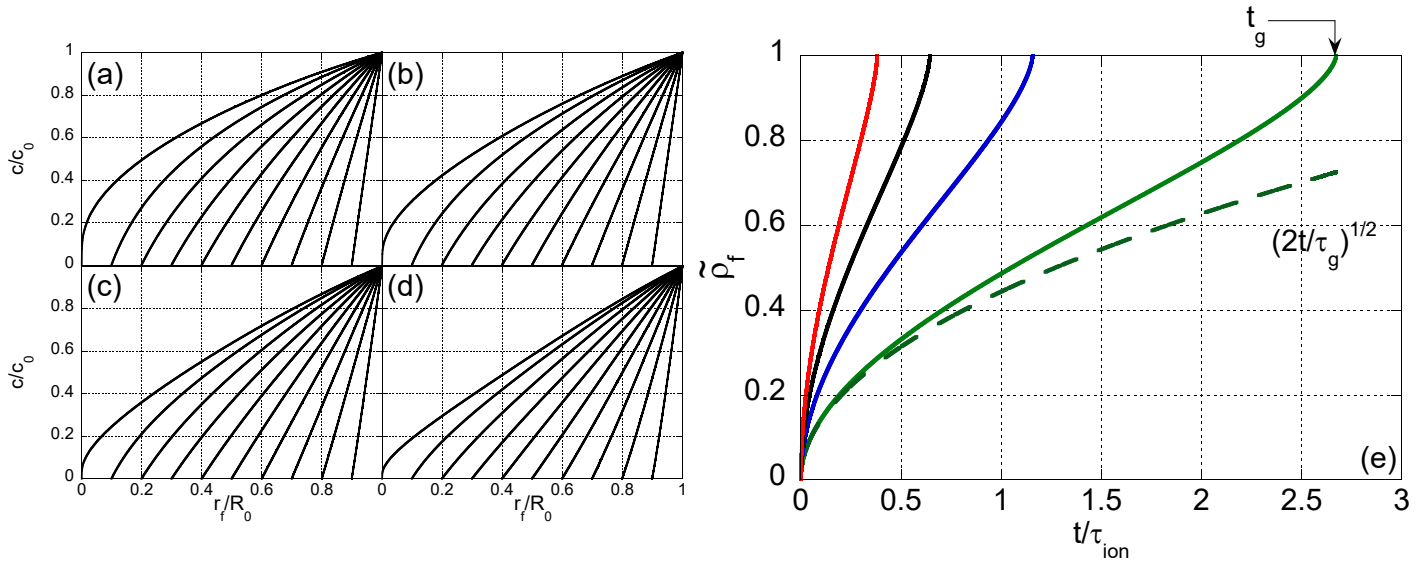

Figure 4 Evolution of the concentration profile c/c_0 as a function of r/R_0 for (a) $c_0/n = 0.1$, (b) $c_0/n = 0.25$, (c) $c_0/n = 0.5$ and (d) $c_0/n = 1$. (e) Full lines : corresponding evolution of the gelation front $\tilde{\rho}_f(t/\tau_{\rm ion})$ with increasing c_0/n from bottom to top. The dashed line is the initial square-root of time regime for the $c_0/n = 0.1$ curve.

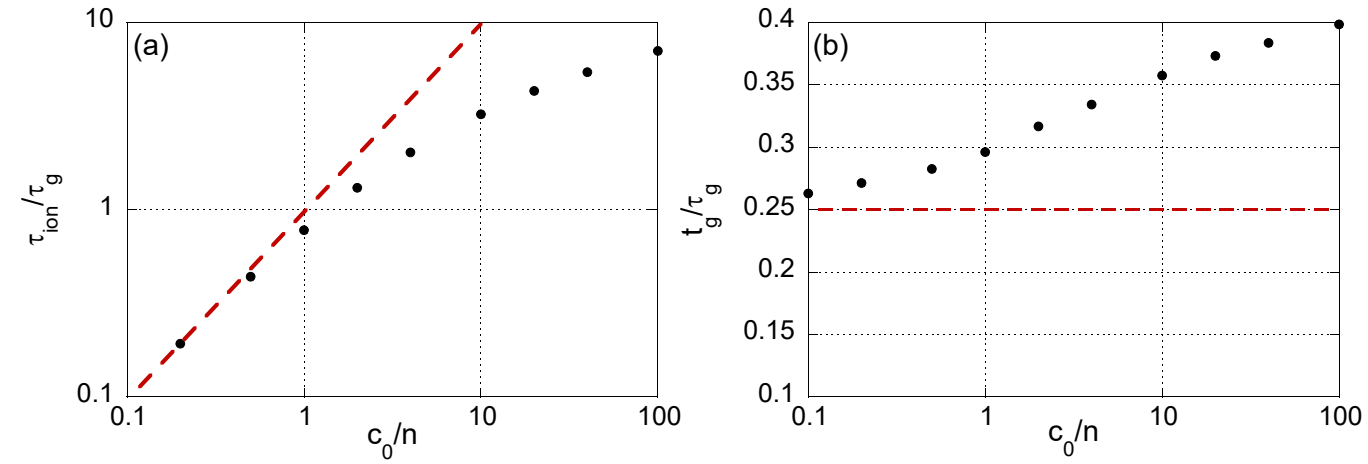

Figure 5 (a) Inverse $\tau_{\rm ion}/\tau_g$ of the characteristic time of the initial square-root advance of the gelation front as a function of the bath concentration c_0/n. (b) Ratio of the gelation time t_g and τ_g as a function of concentration c_0/n. The dashed lines are the quasi-stationary values, which are recovered, as expected, when $c_0/n \ll 1$.

yield meaningful order of magnitudes which, for the sake of the discussion, are sufficient.

All concentrations are proportional to the alginate mass fraction C_A. Numerical values are given for a gel of concentration $C_A = 10$ wt.% for which $C_{\rm res} = 390$ mM. The concentration of condensed sodium ions is $[{\rm Na}^+]_{\rm cond} = C_{\rm res}\theta = 130$ mM. So the concentration of free sodium ions is $[{\rm Na}^+]_{\rm free} = 260$ mM.

3.2 Calcium alginate gels

In presence of calcium ions ($z = 2$), the situation is more complex since part of the ions are chelated in egg-box crosslinks[5]. Note that in an egg-box dimer, chelated calcium ions neutralize half of the bound charges. Thus, the linear charge density of an egg box is the same as that of a free chain. The network is therefore homogeneously prone to counterion condensation.

Let us first assume that all sodium ions, including the condensed ones, have been permuted against calcium ions. Since $\xi > 1/2$, calcium ion condensation proceeds. With $[{\rm Ca}^{2+}]_{\rm cl}$ the concentration of chelated calcium ions, the concentration of the charge sites remaining to be neutralized is

$$c_b' = C_{\rm res} - 2[{\rm Ca}^{2+}]_{\rm cl}$$

The concentration of condensed calcium ions is:

$$[{\rm Ca}^{2+}]_{\rm cond} = c_b'\theta(2)$$

with $\theta(2) \simeq 1/3$ since $\xi \simeq 3/2$. The total concentration of calcium ions prevented from diffusing freely in the gel is therefore:

$$[{\rm Ca}^{2+}]_{\rm loc} = [{\rm Ca}^{2+}]_{\rm cl} + [{\rm Ca}^{2+}]_{\rm cond} = \frac{C_{\rm res} + [{\rm Ca}^{2+}]_{\rm cl}}{3}$$

Assuming that both $[Ca^{2+}]$ chelation and exchange with native, condensed $[Na^+]$ are fast processes, the parameter n in the kinetic model must be identified as $[Na^+]_{loc}$. A lower bound of n would be in that case $[Ca^{2+}]_{loc} > C_{res}/3 = 130$ mM clearly incompatible with the measured value $n \simeq 50$ mM. The calcium condensation hypothesis is therefore questionable.

The issue of *equilibrium* condensation of competing counterions of different valences has been addressed theoretically by Manning[6]. He concluded that the highest valence ions (here Ca^{2+}) condense selectively. However, in our case, some sodium counterions are already condensed in the pregel. Manning insists on the high strength of the Coulombic potential responsible for condensation. It can therefore be expected that the replacement of sodium by calcium ions, although favored by equilibrium thermodynamics, is hindered kinetically. To our knowledge this point has never be addressed, either theoretically or experimentally. In the limit of infinitely long sequestration time of condensed sodium ions, n would be attributable to the sole $[Ca^{2+}]_{cl}$. Due to the chelation stoechiometry in an egg-box, $[Ca^{2+}]_{cl} < C_{res}FG/4$ with $FG = 0.45$ the fraction of G residues. This reads $[Ca^{2+}]_{cl} < 44$ mM. The experimental $n \simeq 50$ mM pleads for densely cross-linked gels with no calcium ion condensation.

3.3 Donnan effect

When Ca^{2+} is the sole counterion species, the global electroneutrality of the network prevents the concentration of free calcium ions inside the gel to be smaller than half the concentration of monovalent charge sites on the network which have not been neutralized by specific chelation or Manning condensation. Consequently, the concentration of calcium ions inside the gel remains larger than outside (Donnan's equilibrium[7]). Assuming that thermodynamical equilibrium has been ultimately reached so that the condensat consists exclusively of calcium ions, and that the concentration of chelated ions is $[Ca^{2+}]_{cl} = C_{res}FG/4$, the minimal amount of free ions inside the gel is:

$$c_{min} = \frac{C_{res}}{2} - C_{res}\frac{1+FG/4}{3} = 0.13\,C_{res}$$

For $C_A = 6$ wt.% (relevant to the solvent swap experiments), $C_{res} = 234$ mM and $c_{min} = 30$ mM. When $c_{swap} \gg c_{min}$, outer and inner concentrations are almost equal and osmotic pressures balance. This is the case in the initial gel prepared with $c_0 = 1$ M. When $c_{swap} \ll c_{min}$, the net osmotic pressure difference approaches $\Pi_{ion} = RTc_{min}$ with R Mayer's constant. This yields $\Pi_{ion} \simeq 80$ kPa.

Notes and references

[1] M. S. Chavez, J. A. Luna and R. L. Garrote, *Journal of food science*, 1994, **59**, 1108–1110.

[2] W. H. Press, S. A. Teukolsky, W. T. Vetterling and B. P. Flannery, *Numerical recipes 3rd edition: The art of scientific computing*, Cambridge university press, 2007.

[3] G. S. Manning, *Berichte der Bunsengesellschaft für physikalische Chemie*, 1996, **100**, 909–922.

[4] G. S. Manning, *The journal of chemical Physics*, 1969, **51**, 924–933.

[5] I. Donati, J. C. Benegas, A. Cesàro and S. Paoletti, *Biomacromolecules*, 2006, **7**, 1587–1596.

[6] G. S. Manning, *The Journal of Physical Chemistry*, 1984, **88**, 6654–6661.

[7] M. Doi, *Soft matter physics*, Oxford University Press, 2013.